Size-Selective Electrochemical Preparation of Surfactant-Stabilized Pd-, Ni- and Pt/Pd Colloids

Manfred T. Reetz,*[a] Martin Winter,[a] Rolf Breinbauer,[a] Thomas Thurn-Albrecht,[b] and Walter Vogel[c]

Dedicated to Professor Jean Normant on the occasion of his 65th birthday

Abstract: A detailed study concerning the size-selective electrochemical preparation of $R_4N^+Br^-$-stabilized palladium colloids is presented. Such colloids are readily accessible using a simple electrolysis cell in which the sacrificial anode is a commercially available Pd sheet, the surfactant serving as the electrolyte and stabilizer. It is shown that such parameters as solvent polarity, current density, charge flow, distance between electrodes and temperature can be used to control the size of the Pd nanoparticles in the range 1.2 – 5 nm. Characterization of the Pd colloids has been performed using transmission electron microscopy (TEM), small angle X-ray scattering (SAXS) and X-ray powder diffractometry (XRD) evaluated by Debye-function-analysis (DFA). Possible mechanisms of particle growth are discussed. Experiments directed towards the size-selective electrochemical fabrication of $(n\text{-}C_6H_{13})_4N^+Br^-$-stabilized nickel colloids are likewise described. Finally, a new strategy for preparing bimetallic colloids (e.g., Pt/Pd nanoparticles) electrochemically is presented, based on the use of a preformed colloid (e.g., $(n\text{-}C_8H_{17})_4N^+Br^-$-stabilized Pt particles) and a sacrificial anode (e.g., Pd sheet).

Keywords: colloids · electrochemistry · palladium · surfactants · transition metals

Introduction

Nanoscale transition metal colloids and clusters are of considerable interest as catalysts in organic and inorganic transformations, as electrocatalysts in fuel cells and as materials with novel electronic, optical and magnetic properties.[1] In many cases the size of the nanoparticles, especially in the range of 1 – 6 nm, strongly influences the catalytic and electronic properties, which is the reason why research efforts directed towards the development of reliable methods for the size-selective preparation of these materials are increasing. Indeed, Bradley's statement in 1994 that "the true control of particle size remains the most attractive goal for the synthetic chemist in the field" is still relevant today.[2, 3] The standard methods for colloid formation are based on the chemical reduction of transition metal salts using such different reducing agent as hydrogen, alcohols, aldehydes, hydrazine, carbon monoxide, hydroxylamines, silanes, borohydrides or electrides in the presence of such stabilizers as special ligands,[1] solvents,[1] polymers[1] or surfactants[1, 4] of the type $R_4N^+X^-$ which prevent undesired agglomeration with formation of metal powders. Generally, the actual size of the nanoparticles obtained varies from system to system, an observation that is not easy to explain, especially in view of the fact that not only the stabilizer, the reducing agent and the nature of the metal are varied, but also other parameters such as solvent, concentration, temperature and reaction time. To make things worse, in some publications experimental details concerning these parameters are not provided.

Truly systematic studies of size-selective syntheses of transition metal colloids are not as common as one would wish.[1] In a series of classical papers Turkevich postulated that the relative rates of two crucial processes determine the size of metal particles, namely that of nucleation and growth.[5a–c] Accordingly, fast nucleation relative to growth tends to result in small particle size. In its most basic form, this postulate is still accepted today.[1, 5d–f] The problem is then reduced to the question of how to identify and how to control the factors which govern the kinetic processes. Nucleation and growth are themselves complicated processes which have been illuminated only in a few select cases, as in Henglein's classical studies of silver and palladium clusters using pulse radiolysis.[6] Accordingly, charged dimers Ag_2^+ (or Pd_2^+) are the first intermediates to be formed. However, in bulk

[a] Prof. Dr. M. T. Reetz, Dr. M. Winter, Dr. R. Breinbauer
Max-Planck-Institut für Kohlenforschung
Kaiser-Wilhelm-Platz 1, 45470 Mülheim/Ruhr (Germany)
Fax: (+49) 208-306-2985
E-mail: reetz@mpi-muelheim.mpg.de

[b] Dr. T. Thurn-Albrecht
Max-Planck-Institut für Polymerforschung
Ackermannweg 10, 55128 Mainz (Germany)

[c] Dr. W. Vogel
Fritz-Haber-Institut der Max-Planck-Gesellschaft
Faradayweg 4 – 6, 14195 Berlin (Germany)

0947-6539/01/0705-1084 $ 17.50+.50/0

preparations of transition metal colloids using other methods it is generally not clear at what particular size the nucleus begins to constitute a new phase. Moreover, following formation of a stable nucleus, various mechanisms for further growth are possible. For example, an "atom by atom" buildup has been discussed, as in photographic emulsions.[7] Such surface catalytic growth also appears to be the primary principle in other processes as well.[8] This also pertains to the formation of $[Bu_4N]_9P_2W_{15}Nb_3O_{32}$-stabilized iridium colloids which has been termed by Finke as "living metal polymerization".[9] Other than the atom by atom mechanism, growth can also be imagined to occur by collision of unstable assemblies of metal atoms (agglomerative growth). The operation of both mechanisms in a given metal colloid preparation is also conceivable.

Returning to purely synthetic aspects, several new approaches to size selectivity have been described recently. For example, older work by the groups of Boutonnet, Nagy, Fendler and others[1] on the preparation of colloidal metals in constrained environments has been elaborated with the emergence of efficient synthetic processes, as in the reduction of transition metal salts in micelles,[10a–g] surfactant emulsions,[10h] liquid crystals,[10i] or polymerized vesicles.[10j] In other work thiolate-encapsulated Au nanoparticles were prepared size-selectively in the range of 2–6 nm by manipulating the thiol-to-gold ratio during the reduction process.[11] In yet a different approach, the nature of reducing alcohols has been systematically varied.[12, 13] Upon changing from methanol to ethanol to isopropanol, the size of Pd or Pt nanoparticles increases, although the range actually observed is rather small.[12] It turned out that the alcohol concentration plays a more dominant role. Oddly enough, the opposite trend, with respect to the nature of the alcohol, was observed upon switching from palladium or platinum to rhodium.[13] One might expect that nanoparticle size should correlate with the reducing power of the system, strong reducing agents leading to fast nucleation relative to growth and therefore to smaller particles. However, this is not evident in these or other systems.[1, 14] The hydrogenation of [Ru(cod)(cot)] (cod = 1,5-cyclooctadiene; cot = 1,3-cyclooctatriene) in mixtures of THF/methanol affords novel types of spongy Ru nanoparticles in the size range of 12 to >500 nm, depending upon the solvent composition.[15] Ligand-stabilized giant metal clusters, the size of which were originally postulated to be characterized by the so-called magic numbers, constitute a special class of nanoparticles.[1d, 16] The discussion concerning the actual factors which govern the size of these monodisperse particles is controversial.[1d, 16, 17]

One of the most definitive synthetic and mechanistic studies with respect to size-selectivity in the preparation of transition metal colloids is the report that the mild thermolysis of palladium salts such as $Pd(NO_3)_2$ in the presence of an excess of tetraalkylammonium carboxylates $R_4N^+(R'CO_2^-)$ as reducing agents and stabilizers makes possible the size-selective preparation of the corresponding Pd nanoparticles in the range 2.5 to 6.8 nm depending upon the electronic nature of the carboxylate anion.[18] Electron-withdrawing substituents in the R′ group of the carboxylate $R'CO_2^-$ correlate with peak potentials $E_{p(ox)}$ and therefore with lower reducing power, which in turn results in slow nucleation and consequently in large particle size. Electron-donating substitutents induce the opposite effects, all other parameters such as temperature, solvent and concentration being constant. Thus, in this system, the controlling element which determines the size of the metal colloids is fairly well understood.[18] The situation is therefore quite different from previous syntheses of $R_4N^+Br^-$ or $R_4N^+Cl^-$-stabilized transition metal colloids in which various types of reducing agents ranging from H_2 to $[Et_3BH]^-R_4N^+$ were employed.[4]

Several years ago we described an electrochemical method for the preparation of $R_4N^+X^-$-stabilized transition metal colloids.[19] Previously, electrochemical processes had been employed in the preparation of insoluble metal powders, usually in aqueous acidic medium.[20] More recently, controlled electrochemical deposition of nanostructured Pd and Cu particles has been reported by Hempelmann.[21a, b] This work is related to that of Penner concerning the electrochemical deposition of silver nanocrystallites on atomically smooth graphite basal plane,[21c] and to the report of Searson and Chien concerning the electrochemical deposition of Ni and Co in polycarbonate templates of nanometer-sized pores created by nuclear track etching.[21d] Other forms of electrochemical metal deposition have been reported by Wiley[21e] and Bartlett.[21f] In contrast, we used a sacrificial anode as the metal source in a simple electrolysis cell, $R_4N^+X^-$ serving as the electrolyte and as the stabilizer in an organic solvent (Scheme 1).[19, 22] This means that the bulk metal at the anode is oxidized to metal cations which then migrate to the cathode where reduction occurs with the formation of ad-atoms. These form clusters which are trapped by the surfactant, a process which results in stabilized colloids rather than insoluble metal powders (Figure 1).

Abstract in German: *Eine detaillierte Studie über die grössenselektive elektrochemische Darstellung von $R_4N^+Br^-$-stabilisierten Palladium-Kolloiden wird beschrieben. Solche Kolloide sind mithilfe einer einfachen Elektrolyse-Zelle leicht zugänglich, in der ein kommerziell erhältliches Pd-Blech als Opferanode dient und das Tensid als Elektrolyt und zugleich als Stabilisator fungiert. Parameter wie Polarität des Solvens, Stromdichte, Ladungsfluss, Abstand zwischen Elektroden sowie Temperatur können herangezogen werden, um die Grösse der Pd-Nanopartikel im Bereich von 1.2 bis 5 nm zu steuern. Die Charakterisierung der Pd-Kolloide erfolgte durch Anwendung der Transmissionselektronenmikroskopie (TEM), Kleinwinkel Röntgen-Streuung (SAXS) sowie Röntgen-Pulver Diffraktometrie (XRD) auf der Basis von Debye-Funktion-Analysen (DFA). Mögliche Mechanismen des Partikelwachstums werden diskutiert. Experimente zur grössenselektiven elektrochemischen Präparation von $(n\text{-}C_6H_{13})_4N^+Br^-$-stabilisierten Nickel-Kolloide werden ebenfalls beschrieben. Schliesslich wird eine neue Strategie zur elektrochemischen Herstellung von bimetallischen Kolloiden, z.B. von Pt/Pd-Nanoteilchen, vorgestellt, die von präformierten Kolloiden [z.B. $(n\text{-}C_8H_{17})_4N^+Br^-$-stabilisierten Pt-Partikeln] und von einer Opferanode (z.B. Pd-Blech) Gebrauch macht.*

Anode: $Met_{bulk} \longrightarrow Met^{n+} + ne^-$

Cathode: $Met^{n+} + ne^- + stabilizer \longrightarrow Met_{coll}/stabilizer$

Sum: $Met_{bulk} + stabilizer \longrightarrow Met_{coll}/stabilizer$

Scheme 1. Electrochemical fabrication of nanosized transition metal colloids (the stabilizer is usually a tetraalkylammonium salt).

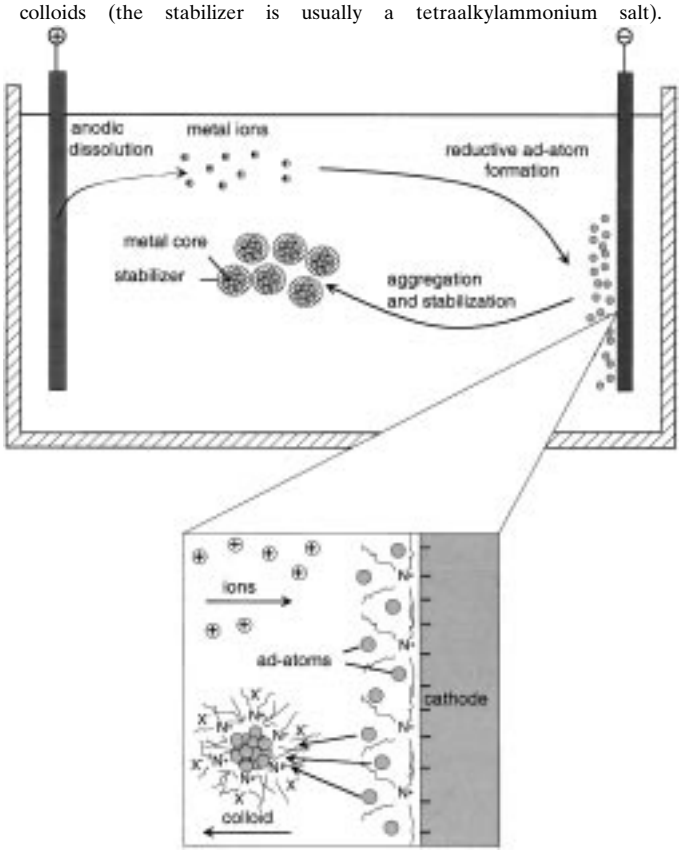

Figure 1. Schematic representation of electrochemical formation of $R_4N^+X^-$-stabilized transition metal colloids.

In the case of palladium colloids a certain degree of size-selectivity was observed, depending upon the current density.[19] Other parameters such as the duration of electrolysis and distance between electrodes were not considered nor were they specifically controlled. The present paper constitutes a careful and systematic study of the effect of these and other factors, including solvent polarity and temperature. It is demonstrated that all of these parameters must be considered in order to obtain synthetically useful results in a simple and reproducible manner.[22] The size of the nanoparticles was determined by transmission electron microscopy (TEM) and small angle X-ray scattering (SAXS). We also report X-ray diffraction (XRD) data and present the results on the basis of a Debye-function-analysis (DFA), thereby shedding some light on the growth mechanism. Finally, the extension to the electrochemical preparation of $R_4N^+X^-$-stabilized nickel colloids and bimetallic Pt/Pd nanoparticles is described.

Results and Discussion

Methods for determining the size of metal nanoparticles: The size of transition metal colloids is generally determined by transmission electron microscopy (TEM).[1] Previously, we published a study of $R_4N^+X^-$-stabilized Pd colloids in which TEM was combined with scanning tunnel microscopy (STM) in order to define the structural relationship between the metal core and the outer stabilizer.[24] It was shown that the ammonium salt $R_4N^+X^-$ forms a monomolecular layer around the Pd clusters. In the present study we again utilize TEM as a standard tool of analysis. In doing so, samples were prepared by simple dip-coating onto conventional Cu grids which were covered by a carbon film. In order to enable a statistically meaningful TEM analysis, at least 300 particles, but in most cases 800–1000 particles on a given grid were considered. In general it can safely be assumed that the values of the nanoparticle size measured by this method following immobilization on a TEM grid also correspond to those prevalent in the actual colloidal solution.

Small angle X-ray scattering (SAXS)[25] was used as a second, independent method to determine the size of the nanoparticles for some of the colloids produced. This method can be used on the original colloidal solutions as prepared, no additional sample preparation involving heterogenization of the sample on a surface being necessary. In addition a very large number of particles is used for the analysis. The solutions considered were in a dilute state; the scattering intensity is then given by Equation (1).

$$I(q) = c_p V_p^2 \Delta\rho^2 |F(q)|^2 \quad (1)$$

where c_p is the number concentration of the particles, V_p the volume of the particles and $\Delta\rho^2$ the electron density difference between the particle and the surrounding solvent. Because of the high electron density of the metallic particles, the scattering signal caused by the surfactants in the solvent can be neglected. The scattering vector is $q = (4\pi/\lambda)\sin\theta$, with 2θ being the scattering angle. $F(q)$ is the form factor of the particles, which for spherical particles of radius R can be given explicitly as Equation (2):

$$F(qR) = 3\frac{\sin qR - qR\cos qR}{(qR)^3} \quad (2)$$

Independent of the exact shape of the particles the form factor can be approximated for small values of q by the Guinier law,[26] [Eq. (3)].

$$|F(q)|^2 \approx \exp(-q^2R_g^2/3) \quad (3)$$

For spherical particles the relation between the radius of gyration R_g and the radius of the sphere R is given by Equation (4):

$$R = \sqrt{\frac{5}{3}}R_g \quad (4)$$

For a polydisperse collection of particles, the result of a SAXS measurement corresponds to a superposition of the contributions from particles of different size. It can be seen from Equation (1), that larger particles contribute more strongly to this average because the scattering power of a particle is proportional to the square of its volume. Consequently, small particles contribute very little to the scattering intensity and

0947-6539/01/0705-1086 $ 17.50+.50/0 Chem. Eur. J. 2001, 7, No. 5

the particle size determined in this way will be larger than the corresponding mean value as determined by TEM.

Solvent effects: In the original version of the electrochemical preparation of $R_4N^+X^-$-stabilized Pd colloids a mixture of acetonitrile (AN) and tetrahydrofuran (THF) was used, but the exact percentage composition was neither varied nor rigorously controlled.[19a] AN is a very polar solvent with a solvent polarity parameter of $E_T = 45.6$, whereas THF is considerably less polar ($E_T = 37.4$).[27] As a first step in understanding and defining the system more closely, we studied the possible influence of solvent polarity by using AN/THF mixtures of precisely defined composition in which the percentage of AN varied from 50% to 0%. All other parameters including the distance between electrodes ($D_E =$ 0.75 mm) were kept constant. The time allowed for electrolysis varied only slightly corresponding to a charge flow (Q) of 0.30–0.44 Ah. The samples obtained in each case were first analyzed by TEM. The results, as summarized in Figure 2,

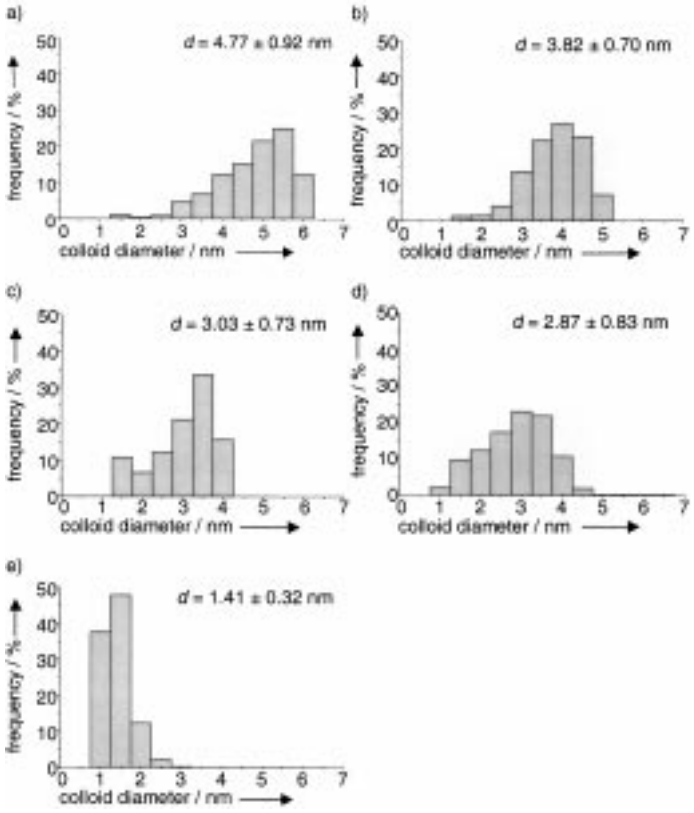

Figure 2. Size distribution (TEM) of electrochemically prepared (n-$C_8H_{17})_4N^+Br^-$-stabilized Pd colloids as a function of the solvent composition ($T = 27\,^\circ C$, $D_E = 0.75$ mm, $I_E = 2.16$ mA cm^{-2}): a) AN/THF = 0.5; b) AN/THF = 0.25; c) AN/THF = 0.17; d) AN/THF = 0.1; e) AN/THF = 0.

show a clear trend: with increasing polarity of the medium, the average size of the Pd nanoparticles increases, the range stretching from 1.4 nm in pure THF to 4.8 nm in a 1:1 mixture of THF and AN. Thus, variation of solvent polarity constitutes a simple means to control the particle size. Upon repeating the experiments several times under identical conditions, a high degree of reproducibility was demonstrated, the average particle diameter varying by less than ±0.25 nm. Isolation in solid form is best performed by adding water to the deep black colloidal solutions which causes the precipitation of the Pd nanoparticles. All samples show a metal content of > 65% and can be fully redispersed in THF if so desired.

The same samples in the form of colloidal solutions were then studied by SAXS. The Guinier analysis was performed in addition to the application of a model based on spheres with a Gaussian distribution in the radius. Not unexpectedly, the size of the particles was found to be systematically larger than the TEM values by a small amount (Figure 3).

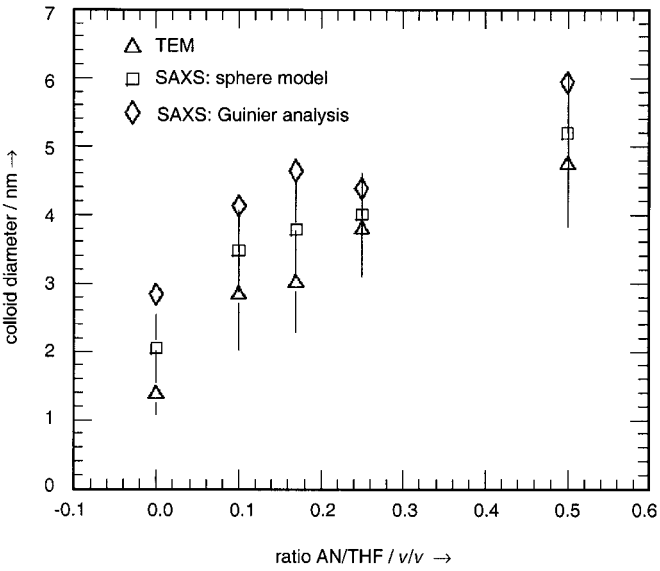

Figure 3. Influence of the solvent composition on the Pd particle size as determined by TEM and SAXS (same samples as in Figure 2).

In order to shed more light on these analyses two scattering curves are shown as an example in Figure 4. The data are taken from the series of experiments corresponding to Figure 3 (ratio AN/THF = 0.17) and from those in which current density was varied (5.41 mA cm^{-2}, charge flow 0.5 Ah; see data presentation below). The diagram shows the scattering curves on a double logarithmic scale, for the upper curve together with a model corresponding to spheres with a Gaussian distribution in the radius. Whereas in the upper curve the minima of the form factor are visible, these cannot be distinguished as clearly in the lower curve, due to polydispersity and limited q range of the instrument. In the inset, a Guinier plot is shown for the same data sets. Here the Guinier law corresponds to a straight line. The broken lines show the corresponding model curves. Since the full analysis of the scattering curves is not applicable to all samples, the Guinier method was used as a consistent way to analyze the data. A comparison between the two methods was made for some selected data sets. The result is as expected: The Guinier analysis gives a value for the size which corresponds to the upper wing of the distribution in case of the full analysis. For the upper curve shown in Figure 4, TEM gives a particle diameter of 3 nm, the full SAXS analysis leads to a value of 3.8 nm and $\sigma = 0.3$ nm. The Guinier value ($d = 4.6$ nm) is even higher. Such limitations concerning the absolute value of the

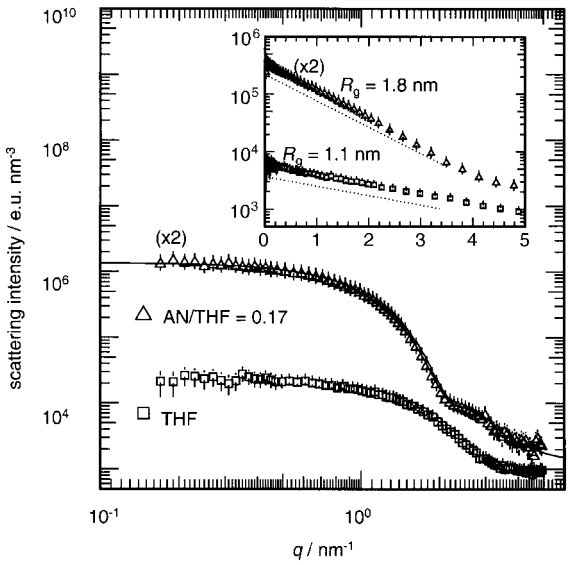

Figure 4. SAXS scattering curves for two selected samples of different size as described in the text. The line corresponds to a fit by a model assuming a polydisperse collection of spheres. In the inset, the data are shown in a Guinier representation. The linear parts of the curves correspond to a Guinier law. The broken lines underneath the data show the corresponding model curves. The resulting radii of gyration are indicated.

particle size must be kept in mind when performing and analyzing scattering experiments using polydisperse samples. Nevertheless, trends in particle size due to different conditions of synthesis are in fact consistent when comparing the TEM and SAXS results.

Effect of charge flow: Subsequent to these initial studies, the possible effect of electrolysis duration as measured by the charge flow (Q) on particle size was investigated. In an exploratory experiment an electrolyte was chosen in which the AN/THF ratio was fixed at 0.17. Interestingly, the particle diameter was found to increase with increasing time (Figure 5). The most pronounced effect occurs in the early phase of electrolysis and levels off after a charge flow of about 0.5 Ah.

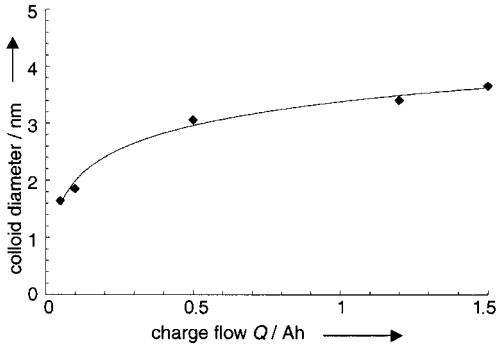

Figure 5. Influence of charge flow Q on Pd particle size (TEM) (solvent AN/THF = 0.17, T = 27 °C, D_E = 0.75 mm, I_E = 2.16 mA cm^{-2}).

The data indicate that the size of the particles is largely determined by a growth process taking place during the synthesis. The details depend on the polarity of the solvent, higher polarity enhancing the probability of further growth. A reduced electrostatic interaction between the metal colloid and the surfactants in a polar surrounding would be a possible explanation for this observation. In a less polar solvent the stabilizing shell would then more effectively shield the particle against further growth. No conclusions can be drawn at this point about the exact mechanism of growth. One possibility is further growth of particles by reaction with ad-atoms or small reactive clusters thereof. A different possible explanation for the variation of particle size with time can be tested, namely an effect due to the changing concentration during the time resolved measurements resulting from the consumption of the ammonium salt as electrolyte and stabilizer during the synthesis. This would mean that the ad-atoms or clusters thereof are not stabilized sufficiently, unlike in the early phase, leading to larger nanoparticles. However, it was easy to exclude this possibility by the following experiments. Electrolysis in THF was repeated in the early part of the process (up to 0.31 Ah), additional $(n\text{-}C_8H_{17})_4N^+Br^-$ being added periodically to compensate for surfactant uptake in its function as a colloid stabilizer. No significant effect on particle size was observed.[22]

The role of current density: Although the size of the Pd nanoparticles can be controlled conveniently by adjusting the AN/THF solvent ratio, the method does have the potential disadvantage that the colloids contain AN. Indeed, even if the solid materials obtained following work-up are subjected to prolonged vacuum by a diffusion pump, some AN remains incorporated, as shown by infrared spectroscopy and mass spectrometric analyses.[22] It is likely that in these systems the surfactant and the solvent AN jointly function in stabilizing the Pd colloids. Although this might be of secondary importance, it is conceivable that the presence of AN may have an adverse effect in certain catalytic applications. Therefore, the search for possible control elements for the size-selective fabrication of $R_4N^+X^-$-stabilized Pd colloids in the absence of AN was continued, current density (I_E) being the first of several parameters to be considered. Upon applying a current density of 2.16 and 5.41 mA cm^{-2} (T = 20 °C; D_E = 5.0 mm; THF pure) for a relatively long electrolysis duration (Q) corresponding to 2.1 Ah, Pd colloids having an average diameter of 2.56 and 1.39 nm, respectively, were obtained. Thus, at higher current density smaller particles are formed. Such a trend is not completely surprising since it is known from the literature on electrochemical metal powder production that the critical radius r_{crit} of clusters of ad-atoms prior to powder formation at the cathode interface is predicted by Equation (5):

$$r_{crit} = \frac{2M\gamma}{nF\eta\rho} \quad (5)$$

where M = molecular weight, γ = surface tension, F = Faraday constant, η = overpotential, ρ = density of the cluster, and n = valency.[28] Accordingly, r_{crit} is inversely dependent on the overpotential η, which in turn is directly related to the current density. This would explain the results. However, due to the observed influence of charge flow on particle size, the state of the matter is considerably more complicated. Indeed, upon recording the particle size as a function of charge flow, a

0947-6539/01/0705-1088 $ 17.50+.50/0 Chem. Eur. J. 2001, 7, No. 5

different behavior was observed at the two current densities applied (2.16 mA cm^{-2} and 5.41 mA cm^{-2}) (Figure 6). At high current density the average diameter of the Pd particles remains approximately constant over the entire electrolysis (Figure 6; Table 1), whereas at low current density particle size increases with time (Figure 6).

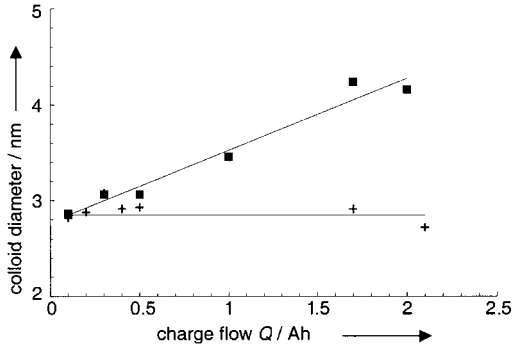

Figure 6. Influence of current density on particle size (SAXS) of (n-$C_8H_{17})_4N^+Br^-$-stabilized Pd colloids at different charge flow Q: Current density = 2.16 mA cm^{-2} (■); current density = 5.41 mA cm^{-2} (+) (T = 20 °C, D_E = 5.0 mm, solvent THF).

Table 1. Influence of charge flow Q on particle size of electrochemically prepared (n-$C_8H_{17})_4N^+Br^-$-stabilized Pd colloids (T = 20 °C, D_E = 0.75 mm, I_E = 5.41 mA cm^{-2}).

Sample	Charge flow Q [Ah]	Pd dissolved [mg]	Current yield [%]	Size (SAXS) [nm]
1	0.1	151	76	2.82
2	0.2	243	61	2.88
3	0.3	313	53	3.08
4	0.4	370	47	2.91
5	0.5	572	58	2.93
6	1.7	861	26	2.93
7	2.1	1006	24	2.72

In fact, at low charge flow the current density has no significant influence on particle size. Moreover, the large particles obtained using a low current density (2.16 mA cm^{-2}) at long electrolysis duration have a bimodal character (d = 2.56 ± 0.9 nm), whereas the Pd colloids having small particles obtained by applying a high current density (5.41 mA cm^{-2}) have a narrow size distribution (d = 1.39 ± 0.49 nm) both experiments being carried out in THF at D_E = 5 mm.[22] The data suggest an enhancement of growth as compared to nucleation under the conditions of low current density. Growth processes do not necessarily have to take place at the electrode. We generally observe a decrease of the current yield with time, as shown in Table 1 for the series of measurements at high current density (5.41 mA cm^{-2}). Here the amount of Pd dissolved was measured after every step. A similar decrease of current yield was observed for syntheses under different conditions. This may be due to the formation of negatively charged Pd colloids which begin to be discharged at the anode. Charged colloids could well participate in a growth process, but since the exact parameters controlling this process are not known at this point, we prefer not to offer a detailed explanation of the observations.

Influence of distance between electrodes: A parameter that was found to have a distinct influence on particle size is the distance between cathode and anode, D_E, which means that care must be taken when constructing the actual electrolysis setup. In two series of experiments a sacrificial Pd anode and an inert Pt anode, each 9.25 cm^2 in area, were placed 0.75 mm and 5.00 mm from one another. A current density of 5.41 mA cm^{-2} was chosen because at this value no time-dependent colloid growth had been observed previously (see above). The results are striking in that at large D_E small particles having a constant size, irrespective of electrolysis duration, are formed, whereas, at small D_E, particle size is larger and increases as electrolysis proceeds (Figure 7). The

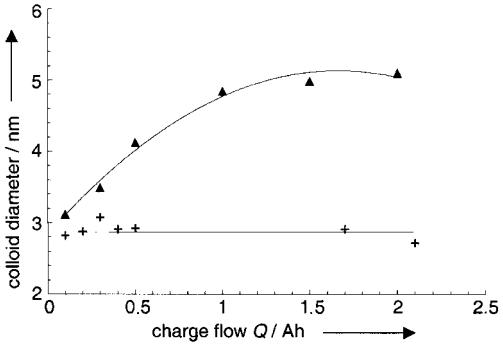

Figure 7. Dependency of particle size (SAXS) of electrochemically prepared (n-$C_8H_{17})_4N^+Br^-$-stabilized Pd colloids on electrode distance (D_E) at different charge flow Q: D_E = 0.75 mm (▲, D_E = 5.0 mm (+) (T = 20 °C, I_E = 5.41 mA cm^{-2}, solvent THF).

statistical evaluation of the TEM results show a relatively broad size distribution in the case of small D_E and almost monodisperse behavior at large D_E. An unambiguous interpretation is difficult because a variety of factors are probably involved, including transport rates and electrophoretic mobilities which are proportional to the fields.[29]

Influence of the nature of the ammonium salt: In order to test whether the $R_4N^+X^-$-stabilized Pd colloids, once formed as stable entities, continue to grow under the electrolysis conditions, the nature of the ammonium salt was varied. Whereas all of the experiments described so far pertain to (n-$C_8H_{17})_4N^+Br^-$-stabilized Pd colloids which are completely soluble in THF, the use of (n-$C_4H_9)_4N^+Br^-$ as an electrolyte and stabilizer would be expected to afford Pd colloids which are largely insoluble in this medium. Indeed, it was observed that under such conditions the (n-$C_4H_9)_4N^+Br^-$-stabilized Pd colloids precipitate during electrolysis, which means that the chance of further growth is limited. Experimentally, it turned out that, in this system, the size of the Pd particles remains almost constant over the entire duration of electrolysis, even at a D_E value of 0.75 mm (Figure 8).

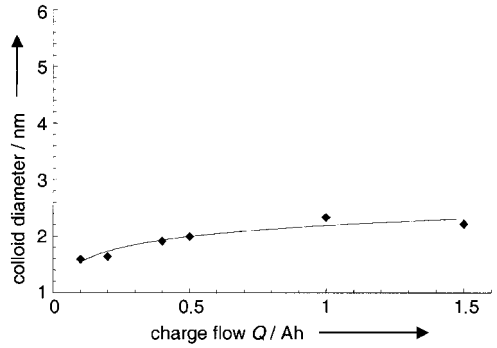

Figure 8. Dependency of particle size (TEM) of $(n\text{-}C_4H_9)_4N^+Br^-$-stabilized Pd colloids as a function of charge flow Q ($T = 27\,^\circ C$, $D_E = 0.75$ mm, $I_E = 5.41$ mA cm^{-2}, solvent THF).

Temperature effect: Finally, the possible effect of temperature on the size of the $(n\text{-}C_8H_{17})_4N^+Br^-$-stabilized Pd colloids was studied. In a typical series of experiments electrolyses were performed at 15 °C, 40 °C and 60 °C ($D_E = 0.75$ mm, $I_E = 5.41$ mA cm^{-2}, solvent THF). The results show that particle size increases with increasing temperature as shown by two independent methods, namely TEM and SAXS analyses (Figure 9). Thus, it is a simple matter to vary the average

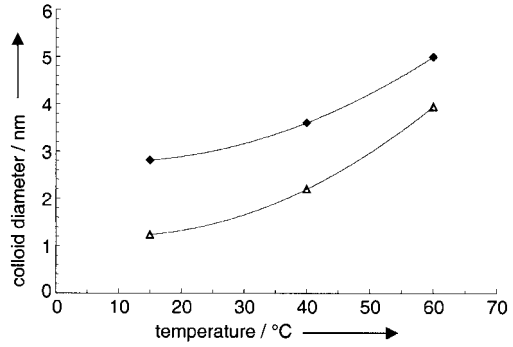

Figure 9. Effect of temperature on the size of electrochemically prepared $(n\text{-}C_8H_{17})_4N^+Br^-$-stabilized Pd colloids: SAXS (◆), TEM (△) ($D_E = 0.75$ mm, $I_E = 5.41$ mA cm^{-2}, solvent THF).

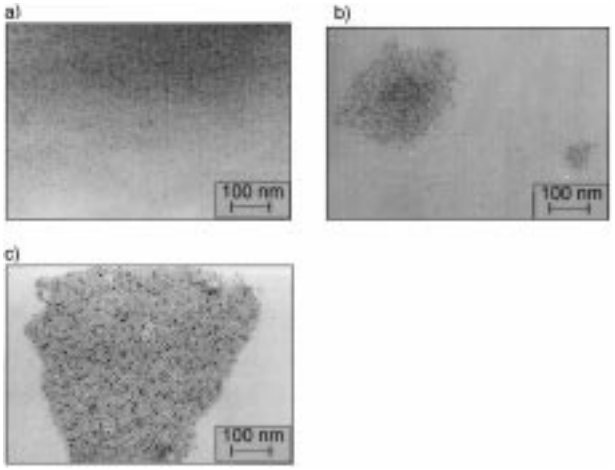

Figure 10. TEM images of $(n\text{-}C_8H_{17})_4N^+Br^-$-stabilized Pd colloids obtained electrochemically ($D_E = 0.75$ mm, $I_E = 5.41$ mA cm^{-2}, $Q = 0.5$ Ah; solvent THF) at a) 15 °C; b) 40 °C; c) 60 °C.

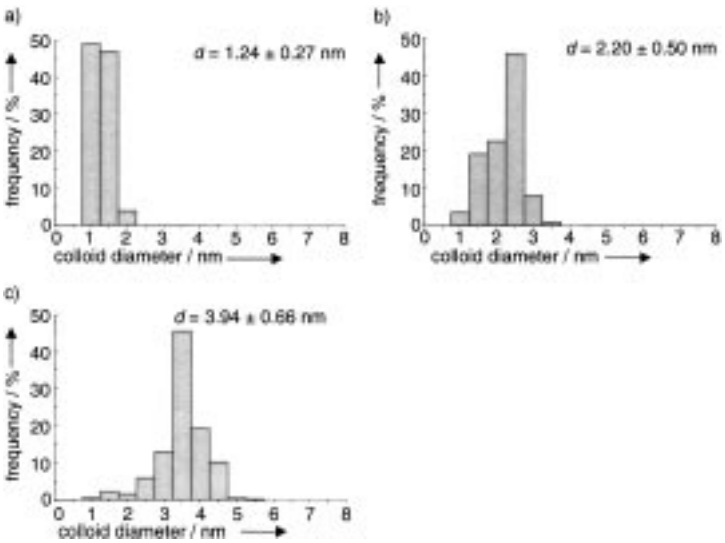

Figure 11. Size distribution (TEM) of electrochemically prepared ($D_E = 0.75$ mm, $I_E = 5.41$ mA cm^{-2}, $Q = 0.5$ Ah) $(n\text{-}C_8H_{17})_4N^+Br^-$-stabilized Pd colloids at a) 15 °C; b) 40 °C; c) 60 °C.

particle size in the range 1.24 to 3.94 nm (values from TEM). Moreover, the respective size distribution is rather narrow, as demonstrated in Figures 10 and 11. The results can be explained by postulating higher diffusion, migration and dissociation rate of the tetraalkylammonium palladate intermediates at elevated temperatures, as well as decreasing viscosity of the medium leading among other things to a lower cathodic overpotential. Of course, other factors such as higher desorption rate of the stabilizer from the particle surface at higher temperatures may also play a role.

Simultaneous variation of two parameters: Obviously, in the quest to find ways to control particle size of the $(n\text{-}C_8H_{17})_4N^+Br^-$-stabilized Pd colloids, it is possible to combine the various parameters delineated above. One of several possibilities is illustrated here, namely to change from the usual room temperature to 60 °C and to vary the duration of electrolysis, whilst keeping other factors constant ($D_E = 0.75$ mm, $I_E = 5.41$ mA cm^{-2}). Not unexpectedly, the average particle size as determined by TEM varies in a defined and reproducible manner: $d = 1.93 \pm 0.6$ nm (at $Q = 0.2$ Ah); $d = 3.94 \pm 0.66$ nm (at $Q = 0.5$ Ah) and $d = 4.28 \pm 0.99$ nm (at $Q = 1.0$ Ah). The statistical evaluation[22] again points to a narrow size distribution which is typical of the electrochemical preparation method.

Further characterization: Although no detailed mechanistic studies regarding colloid formation were carried out, all of the observations are consistent with a growth mechanism involving $R_4N^+X^-$-stabilized particles. However, some formation of new nucleation points during electrolysis and therefore of new colloids may well occur parallel to growth. In order to gain more information of the structural nature of the Pd colloids and possibly of their mode of formation, X-ray powder diffractometry (XRD) was applied.[30] Because the evaluation of XRD data obtained from particles in the size range < 4 nm is problematic, the Debye-function-analysis (DFA) of the XRD spectra was employed.[31] An XRD/DFA study of this

0947-6539/01/0705-1090 $ 17.50+.50/0 *Chem. Eur. J.* **2001**, *7*, No. 5

kind has previously been carried out successfully, the Euro Pt-1 catalyst (6.3% Pt on SiO_2) and the Schmid cluster $Au_{55}(PPh_3)_{12}Cl_6$ serving as the nanoparticles.[31] In the present study a Pd colloid prepared at 60 °C using an electrode distance (D_E) of 0.75 mm and a current density (I_E) of 5.41 mA cm^{-2} was studied by XRD/DFA, the sample being isolated by precipitation with water after 0.2 Ah. The corresponding XRD spectrum and the DFA fit are reproduced in Figure 12.

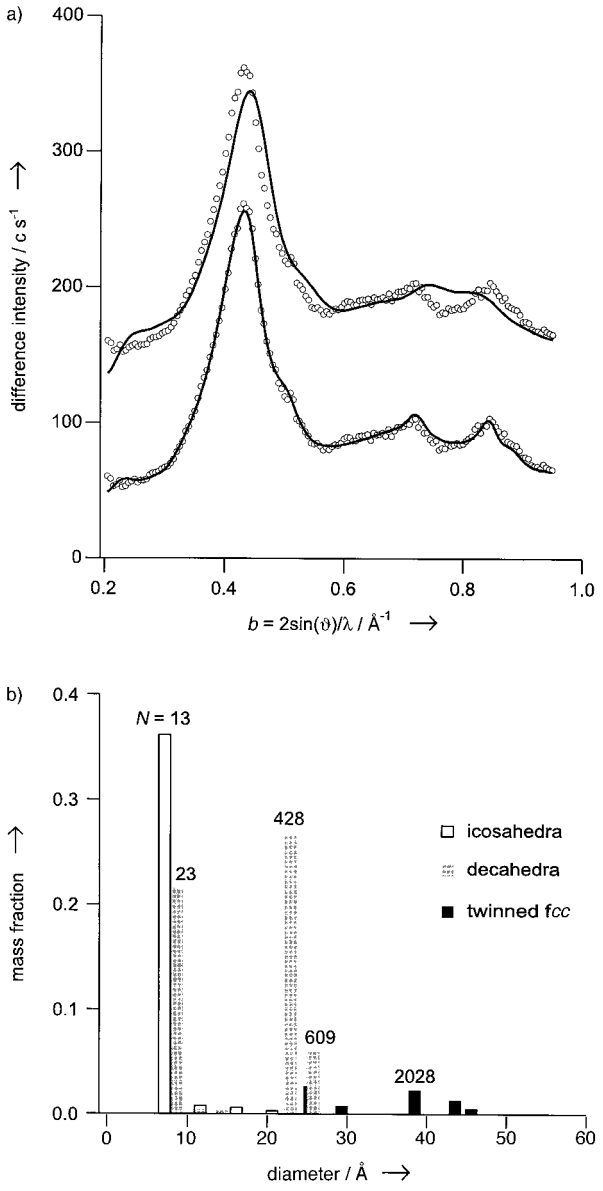

Figure 12. a) Experimental (○) and DFA-fitted (——) XRD spectra of a (n-$C_8H_{17})_4N^+Br^-$-stabilized Pd-colloid ($D_E = 0.75$ mm, $I_E = 5.41$ mA cm^{-2}, $Q = 0.20$ Ah, $T = 60$ °C, solvent THF); b) particle size distribution of the same sample.

The method for analyzing X-ray diffractograms from complex systems of nanoparticles using model Debye functions (DFA) is based on the results of many consistent TEM studies. They confirm the existence of so-called multiply twinned particles (MTPs) with non-periodic five-fold symmetry of decahedral or icosahedral shape for metal nanoparticles. It is also well known that with increasing size there is a transition from these five-fold symmetric particles to the regular bulk structure with some twinning defects. For the simulations we used a sequence of increasing size for the different particle types. Some of the features of the diffraction curves are so specific and so characteristic that they can only be simulated by, for example, a fraction of larger *fcc*-type particles. This is, in fact, the case for the palladium system studied here: the two "narrow" peaks at $b = 0.73$ Å^{-1} and at $b = 0.85$ Å^{-1}, as well as the shoulders at the high angle wings of peak 1 and 3 of Figure 12a are typical fcc features. To underline this statement we show two simulations that differ only in one point: the top curve excludes fcc-type particles (shown with offset), and the lower curve includes the twinned *fcc*-type model Debye functions (size range 25–50 Å). The necessary improvement is evident. The related *R* factor is improved by a factor of 3. The fraction by mass of the *fcc* particles is in the order of 10% (Figure 12b).

Both groups of particles, of the smaller MTP-type and of the larger *fcc*-type, have been given an individual scaling parameter, which refers to a possible contraction/expansion against the bulk palladium near neighbor distance. The method has been described in a recent paper on nanocrystalline gold.[30c] Surprisingly, here an interatomic distance of 2.96 Å for the smaller MPT particles is found, corresponding to an extreme expansion of 7.5% relative to the value in bulk palladium (2.75 Å). Such an increase could be caused by the incorporation of "foreign" atoms or ions,[32] although this is a matter of speculation. For the larger *fcc* fraction the Pd–Pd distance is essentially the same as in the bulk material. Noteworthy is the fact that the DFA-derived mean particle diameter of 0.8 nm is significantly smaller than the value determined by TEM (1.93 ± 0.6 nm). At least part of this discrepancy is due to the fact that particles less than 1 nm in size are inefficiently detected by TEM. However, it is possibly also a result of the fact that the (n-$C_8H_{17})_4N^+Br^-$-stabilized Pd colloids are not single crystals. Indeed, they are composed of smaller primary particles, the sizes of which are reflected in the DFA analysis. Further support for this structural feature is derived from the finding that the integral line widths as determined by Pearson-VII functions increase significantly with the reflex order. In general, such broadening can be explained on the basis of an overlap of an approximately constant contribution related to the particle size and contributions due to irregularities in stacking and/or to micro-strain. This, again, is in line with the formation of polycrystalline secondary particles and the thereby associated state of strain at the grain boundaries of the primary particles. The structural knowledge derived from these studies indicate that the size-selective process is based on a growth mechanism which is characterized by coalescence of once-formed stabilized colloids with smaller ensembles of reactive palladium atoms formed during electrolysis. Control experiments clearly showed that heating the colloids (e.g., 1–2 nm sized samples) alone without applying electrochemical conditions does not result in particle growth.

In spite of the fact that the samples were isolated and handled in air, significant oxidation of the Pd atoms in the

core of the $(n\text{-}C_8H_{17})_4N^+Br^-$-stabilized colloids can be excluded. Thus, there is little correspondence between the observed diffraction reflexes of the Pd-colloid and those of calculated hypothetical 5 nm-sized PdO nanoparticles (Figure 13). A slight shoulder at the (111) reflex of the colloid indicates a small degree of oxidation, probably at the surface of the Pd core.

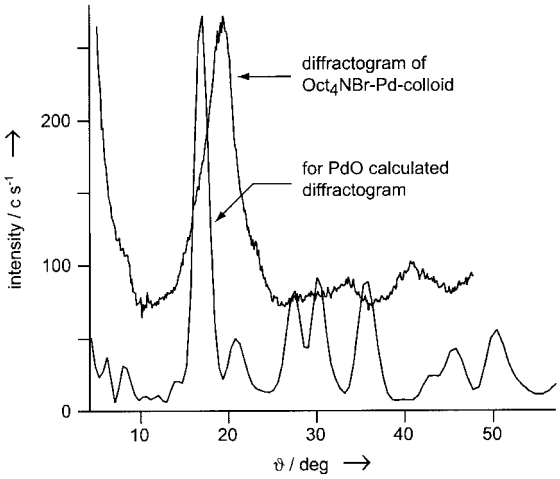

Figure 13. Comparison of the experimental XRD spectrum of an electrochemically prepared $(n\text{-}C_8H_{17})_4N^+Br^-$-stabilized Pd colloid ($D_E = 0.75$ mm, $I_E = 5.41$ mA cm^{-2}, $Q = 0.2$ Ah, $T = 60\,^\circ$C, solvent THF) with the calculated spectrum of a PdO colloid.

Studies concerning Ni and Pt/Pd colloids: In further experiments, it was of interest to see if the effects observed in the size-selective preparation of palladium colloids also operate in the case of other transition metals.[19c] For this purpose the same experimental setup and conditions were employed, except that the Pd anode was replaced by a sacrificial nickel anode.[19c] In this case, $(n\text{-}C_6H_{13})_4N^+Br^-$ served as the electrolyte and the stabilizer in THF. Three different experiments were carried out in which several of the parameters which had previously been shown to be instrumental in determining the size of the Pd colloids were varied. Electrolysis at 60 °C with $D_E = 0.75$ mm, $I_E = 5.41$ mA cm^{-2} and $Q = 0.90$ Ah led to Ni colloids with a mean diameter of 2.9 ± 0.82 nm. Upon lowering the temperature to 20 °C and increasing the electrode distance to $D_E = 5.41$ mm, while keeping I_E (5.41 mA cm^{-2}) and Q (0.90 Ah) constant, considerably smaller sized ($d = 1.16 \pm 0.22$ nm) particles were obtained. This corresponds fully to the trends observed previously in the fabrication of the Pd analogues. In order to see if current density also influences the size of the Ni particles, the third experiment was carried out with I_E being adjusted to 2.16 mA cm^{-2}, all other conditions being the same as in the preparation of the second sample. Indeed, $(n\text{-}C_6H_{13})_4N^+Br^-$-stabilized Ni colloids were obtained having a larger diameter (1.71 ± 0.39 nm), in line with the effect previously observed in the case of the Pd colloids. Yasuhara and Sakamoto have also used the electrochemical method to prepare Ni colloids, in this case the stabilizer being $(n\text{-}C_4H_9)_4N^+BF_4^-$.[33] It should be noted that exploratory experiments using other sacrificial anodes such as Co,[34] Fe,[19c] Cu,[19c] Ag,[19c] Ti,[35] and Au[19c] were also successful, although in some cases the colloids were not as stable as those derived from Pd or Ni. A more detailed study of the use of Au sheets as sacrificial anodes and special tetraalkylammonium salts as electrolytes and stabilizers showed that shape-selectivity in the form of rodlike clusters is possible.[36] Thus, our electrochemical transition metal colloid synthesis seems to have a fairly broad scope.

Finally, it was of interest to see if the electrochemical method described herein can be extended to include the preparation of bimetallic colloids. Previously, we employed an electrolysis setup based on two sacrificial anodes (e.g., Pd and Ni sheets, and an inert cathode).[37] Alternatively, we have shown that two transition metal salts can be reduced electrochemically in the presence of tetraalkylammonium *acetates*, the latter serving as the electrolyte, the stabilizer and as the reductant oxidized at the anode.[37] In the present study we developed a third strategy, namely to start with a preformed colloid derived from one metal and to graft on a second metal electrochemically. Experimentally we started with an $(n\text{-}C_8H_{17})_4N^+Br^-$-stabilized platinum colloid having a metal content of 86% and an average particle size of 3.8 nm.[39] It was added to an electrolysis cell containing a 0.1 M solution of the electrolyte $(n\text{-}C_8H_{17})_4N^+Br^-$ in THF. An inert Pt cathode and a sacrificial Pd anode were chosen as the electrodes ($D_E = 0.75$ mm, $I_E = 5.41$ mA cm^{-2}, $T = 60\,^\circ$C). After a charge flow of $Q = 0.5$ Ah, a sample was taken for TEM analysis. This showed the presence of nanoparticles having an average size of 4.27 ± 0.81 nm. After a charge flow of $Q = 1.0$ Ah electrolysis was terminated, resulting in Pt/Pd colloids having an average size of 4.94 ± 0.79 nm as determined by TEM.[22] EDX-spot analysis of 13 individual particles clearly demonstrated the existence of true Pt/Pd colloids, only two of the particles consisting solely of Pd atoms (Table 2). Thus, these results show that our electrolysis allows for a graft process.[8, 9, 40] Bimetallic colloids are therefore accessible by using a given starting metal colloid and the appropriate sacrificial anode as the source of the second metal.

Table 2. EDX-spot analyses of individual nanoparticles of an $(n\text{-}C_8H_{17})_4N^+Br^-$-stabilized Pt/Pd colloid.

Single particle[a]	Pt [atom %]	Pd [atom %]	percentage Pd [atom %]
1	32.23	19.15	37.27
2	15.24	12.00	44.05
3	–	27.85	100
4	18.72	20.68	52.48
5	14.85	46.85	75.93
6	27.54	22.43	44.86
7	30.76	15.38	33.33
8	32.86	28.30	46.27
9	31.03	48.68	61.07
10	25.99	14.38	35.62
11	–	22.38	100
12	24.46	16.78	40.68
13	9.35	29.22	75.75

[a] EDX beam diameter: ≈ 4 nm.

0947-6539/01/0705-1092 $ 17.50+.50/0 *Chem. Eur. J.* **2001**, *7*, No. 5

Conclusion

In this study we have explored and defined the parameters which are important for controlling size-selectivity in the electrochemical fabrication of $R_4N^+X^-$-stabilized nanoscale palladium and nickel colloids. These include solvent polarity, current density, charge flow, distance between electrodes and temperature. It is thus possible to control the size of the metal colloids in the range of 1.2–5 nm. The combination of TEM, SAXS and XRD/DFA was used to characterize the colloids and to gain preliminary information concerning the growth mechanism of particle formation. All present evidence points to a growth mechanism in which coalescence of $R_4N^+Br^-$-stabilized metal colloids with smaller ensembles of reactive metal atoms dominates. Bimetallic colloids are accessible by starting with a given metal colloid and grafting the second metal onto it electrochemically, the bimetallic character being demonstrated by EDX spot analyses. It remains to be seen if the control elements described in this study are also crucial in our alternative electrochemical preparation of $R_4N^+X^-$-stabilized transition metal colloids according to which metal salts such as $PtCl_2$, $Pd(OAc)_2$, $RuCl_3$, $OsCl_3$ or $Mo_2(OAc)_4$ rather than sacrificial anodes, serve as the metal source.[38]

Experimental Section

Analytical instruments: Transmission electron microscopes (TEM): Hitachi HF 2000 (200 kV) and Siemens Elmiskop (80 kV); small angle X-ray scattering (SAXS): Kratky Kleinwinkelkamera (the algorithm of Strobl was used for deconvolution of slit smeared data[23]); X-ray powder diffractometer (XRD): Huber-Guinier diffractometer.

Chemicals: All of the chemicals that were used are commercially available. Tetraoctylammonium bromide (98%, Fluka), tetrahexylammonium bromide (>99%, Fluka) and tetrabutylammonium bromide (>98%, Fluka) were dissolved in dry THF, the solvent removed in vacuo and the solids dried at 40 °C for 48 h at high vacuum. Acetonitrile was distilled over KOH/$KMnO_4$. THF was distilled over sodium tetraethyl alanate and stored under argon.

Electrolysis cell: Commercially available titration vessels having a volume of 90 mL were modified in the following way: A vessel (Metrohm 6.1415.220) was equipped with a Teflon lid (Metrohm 6.1414.030) having two connections for the electrodes and one for inert gas, an opening for adding solid materials or for a reflux condenser, as well as two openings for adding or taking samples of electrolytes. A commercially available platinum sheet (3.7×2.5 cm^2 area and 0.05 mm thick) served as the inert cathode. Commercially available palladium (or nickel) sheets (3.7×2.5 cm^2 area and 1.0 cm thick) were used as sacrificial anodes. Before use, the electrodes were cleaned with scouring powder and washed with water, acetone and toluene.

Electrolyses: Before actual use the electrolysis cell was dried for several hours at 70 °C in a drying oven and subsequently cooled in an argon stream. The electrolyte was added through an appropriate hose under inert gas (Ar) conditions. The openings were closed with rubber stoppers. For the galvanostatic electricity supply a simple commercially available instrument (Uniwatt NG306) was employed. During electrolysis, the cell was submerged in an ultrasonic cleaning bath (Bandelin Sonorex Super RK 102H). Thermostatization was ensured by cooling elements of an external aggregate (Haake N3 or Lauda UKT 350). In the case of electrolyses at temperatures above 40 °C, a water-cooled reflux condenser was used. In order to take samples during electrolysis, a syringe was employed, and 1–4 mL samples were placed in an argon-filled flask equipped with a Teflon stopper. In those cases in which the palladium consumption was periodically determined during the electrolysis, charge flow was interrupted for a short time, the cell was opened, and the anode was washed with acetone and finally weighed. It was then dried at 70 °C for a short time and re-inserted into the electrolysis cell under an atmosphere of argon. The total interruption took about 5 min.

[1] Reviews on transition metal colloids and nanoparticles: a) *Clusters and Colloids*: *From Theory to Applications* (Ed.: G. Schmid), VCH, Weinheim, **1994**; b) *Nanoparticles and Nanostructured Films* (Ed.: J. H. Fendler), Wiley-VCH, Weinheim, **1998**; c) A. Henglein, *Ber. Bunsenges. Phys. Chem.* **1997**, *101*, 1562–1572; d) G. Schmid, L. F. Chi, *Adv. Mater.* **1998**, *10*, 515–526; e) S. C. Davis, K. J. Klabunde, *Chem. Rev.* **1982**, *82*, 153–208; f) G. Schön, U. Simon, *Colloid Polym. Sci.* **1995**, *273*, 101–117, and G. Schön, U. Simon, *Colloid Polym. Sci.* **1995**, *273*, 202–218; g) J. M. Thomas, *Pure Appl. Chem.* **1988**, *60*, 1517–1528; h) J. D. Aiken, R. G. Finke, *J. Am. Chem. Soc.* **1998**, *120*, 9545–9554; i) review of transmission electron microscopy of shape-controlled transition metal nanoparticles: Z. L. Wang, *J. Phys. Chem. B* **2000**, *104*, 1153–1175.

[2] J. S. Bradley in *Clusters and Colloids*: *From Theory to Applications* (Ed.: G. Schmid), VCH, Weinheim, **1994**, pp. 459–544.

[3] See for example: a) K. R. Brown, D. G. Walter, M. J. Natan, *Chem. Mater.* **2000**, *12*, 306–313; b) Y. Zhou, C. Y. Wang, Y. R. Zhu, Z. Y. Chen, *Chem. Mater.* **1999**, *11*, 2310–2312; c) M. Harada, K. Asakura, N. Toshima, *J. Phys. Chem.* **1994**, *98*, 2653–2662; d) T. S. Ahmadi, Z. L. Wang, T. C. Green, A. Henglein, M. A. El-Sayed, *Science* **1996**, *272*, 1924–1926; e) J. C. Ziegler, G. E. Engelmann, D. M. Kolb, *Z. Phys. Chem.* **1999**, *208*, 151–166; f) A. B. R. Mayer, J. E. Mark, *J. Polym. Sci. Part A*: *Polym. Chem.* **1997**, *35*, 3151–3160; g) N. A. Dhas, C. P. Raj, A. Gedanken, *Chem. Mater.* **1998**, *10*, 1446–1452; h) W. Yu, H. Liu, *Chem. Mater.* **1998**, *10*, 1205–1207; i) J.-D. Grunwaldt, C. Kiener, C. Wögerbauer, A. Baiker, *J. Catal.* **1999**, *181*, 223–232; j) L. M. Liz-Marzan, M. Giersig, P. Mulvaney, *Langmuir* **1996**, *12*, 4329–4335; k) A.-M. L. Jackelen, M. Jungbauer, G. N. Glavee, *Langmuir* **1999**, *15*, 2322–2326; l) A. Miyazaki, Y. Nakano, *Langmuir* **2000**, *16*, 7109–7111; m) K. R. Brown, D. G. Walter, M. J. Natan, *Chem. Mater.* **2000**, *12*, 306–313; n) J. Zhu, S. Liu, O. Palchik, Y. Koltypin, A. Gedanken, *Langmuir* **2000**, *16*, 6396–6399; o) W. P. McConnell, J. P. Novak, L. C. Brousseau III, R. R. Fuierer, R. C. Tenent, D. L. Feldheim, *J. Phys. Chem. B* **2000**, *104*, 8925–8930.

[4] Surfactant stabilizers of the type $R_4N^+X^-$ have been used particularly often; see for example: a) J. Kiwi, M. Grätzel, *J. Am. Chem. Soc.* **1979**, *101*, 7214–7217; b) Y. Sasson, A. Zoran, J. Blum, *J. Mol. Catal.* **1981**, *11*, 293–300; c) M. Boutonnet, J. Kizling, P. Stenius, G. Maire, *Colloids Surf.* **1982**, *5*, 209–229; d) N. Toshima, T. Takahashi, H. Hirai, *Chem. Lett.* **1985**, 1245–1248; e) M. Boutonnet, J. Kizling, R. Touroude, G. Maire, P. Stenius, *Appl. Catal.* **1986**, *20*, 163–177; f) K. Meguro, M. Torizuka, K. Esumi, *Bull. Chem. Soc. Jpn.* **1988**, *61*, 341–345; g) J. Wiesner, A. Wokaun, H. Hoffmann, *Prog. Coll. Polym. Sci.* **1988**, *76*, 271–277; h) N. Satoh, K. Kimura, *Bull. Chem. Soc. Jpn.* **1989**, *62*, 1758–1763; i) H. Bönnemann, W. Brijoux, R. Brinkmann, E. Dinjus, T. Joussen, B. Korall, *Angew. Chem.* **1991**, *103*, 1344–1346; *Angew. Chem. Int. Ed. Engl.* **1991**, *30*, 1312.

[5] a) J. Turkevich, P. C. Stevenson, J. Hillier, *Discuss. Faraday Soc.* **1951**, 55–75; b) J. Turkevich, *Gold Bull.* **1985**, *18*, 86–91; c) J. Turkevich, G. Kim, *Science* **1970**, *169*, 873–879; d) for extensive literature concerning alternative theoretical models see ref. [1h]; see also: e) A. I. Kirkland, P. P. Edwards, D. A. Jefferson, D. G. Duff, *Ann. Rep. Prog. Chem*, *Sect. C*: *Phys. Chem.* **1991**, *87*, 247–304; f) D. G. Duff, A. Baiker, P. P. Edwards, *Langmuir* **1993**, *9*, 2301–2309.

[6] a) A. Henglein, *Top. Curr. Chem.* **1988**, *143*, 113–180; b) M. Michaelis, A. Henglein, *J. Phys. Chem.* **1992**, *96*, 4719–4724; c) A. Henglein, D. Meisel, *Langmuir* **1998**, *14*, 7392–7396; d) A. Henglein, M. Giersig, *J. Phys. Chem. B* **1999**, *103*, 9533–9539; e) see also Papirer's study on the thermolysis of dicobalt octacarbonyl in constrained environment in which the kinetics of nucleation and growth were monitored: E. Papirer, P. Horny, H. Balard, R. Anthore, C. Petipas, A. Martinet, *J. Colloid Interface Sci.* **1983**, *94*, 220–228.

[7] a) R. B. Pontius, R. G. Willis, *Photogr. Sci. Eng.* **1973**, *17*, 326–333; b) G. Bredig, *Angew. Chem.* **1898**, *11*, 951–954.

[8] a) D. G. Duff, A. Baiker in *Preparation of Catalysts VI*: *Scientific Bases for the Preparation of Heterogeneous Catalysts*, *Vol. 91*, *Stud. Surf. Sci. Catal.* (Eds.: G. Poncelet, J. Martens, B. Delmon, P. A. Jacobs,

P. Grange), Elsevier, Amsterdam, **1995**, pp. 505 – 512; b) K. R. Brown, M. J. Natan, *Langmuir* **1998**, *14*, 726 – 728; c) H. Weller, *Angew. Chem.* **1993**, *105*, 43 – 55; *Angew. Chem. Int. Ed. Engl.* **1993**, *32*, 41 – 53.
[9] M. A. Watzky, R. G. Finke, *J. Am. Chem. Soc.* **1997**, *119*, 10382 – 10400.
[10] a) M. P. Pileni, *Ber. Bunsenges. Phys. Chem.* **1997**, *101*, 1578 – 1587; b) M. Antonietti, F. Gröhn, J. Hartmann, L. Bronstein, *Angew. Chem.* **1997**, *109*, 2170 – 2173; *Angew. Chem. Int. Ed. Engl.* **1997**, *36*, 2080 – 2083; c) A. Taleb, C. Petit, M. P. Pileni, *Chem. Mater.* **1997**, *9*, 950 – 959; d) M. A. Markowitz, G.-M. Chow, A. Singh, *Langmuir* **1994**, *10*, 4095 – 4102; e) K. Kurihara, J. H. Fendler, I. Ravet, J. B. Nagy, *J. Mol. Catal.* **1986**, *34*, 325 – 335; f) S. Puvvada, S. Baral, G. M. Chow, S. B. Qadri, B. R. Ratna, *J. Am. Chem. Soc.* **1994**, *116*, 2135 – 2136; g) A. B. R. Mayer, J. E. Mark, R. E. Morris, *Polym. J.* **1998**, *30*, 197 – 205; h) T. Hanaoka, T. Hatsuta, T. Tago, M. Kishida, K. Wakabayashi, *Appl. Catal. A* **2000**, *190*, 291 – 296; i) J. H. Ding, D. L. Gin, *Chem. Mater.* **2000**, *12*, 22 – 24; j) M. A. Markowitz, G.-M. Chow, A. Singh, *Langmuir* **1994**, *10*, 4095 – 4102.
[11] a) M. M. Maye, W. Zheng, F. L. Leibowitz, N. K. Ly, C.-J. Zhong, *Langmuir* **2000**, *16*, 490 – 497; b) M. Brust, M. Walker, D. Bethell, D. J. Schiffrin, R. Whyman, *J. Chem. Soc. Chem. Commun.* **1994**, 801 – 802; c) J. Fink, C. J. Kiely, D. Bethell, D. J. Schiffrin, *Chem. Mater.* **1998**, *10*, 922 – 926; d) R. H. Terrill, T. A. Postlethwaite, C. Chen, C.-D. Poon, A. Terzis, A. Chen, J. E. Hutchison, M. R. Clark, G. Wignall, J. D. Londono, R. Superfine, M. Falvo, C. S. Johnson, Jr., E. T. Samulski, R. W. Murray, *J. Am. Chem. Soc.* **1995**, *117*, 12537 – 12548; e) M. J. Hostetler, C.-J. Zhong, B. K. H. Yen, J. Anderegg, S. M. Gross, N. D. Evans, M. Porter, R. W. Murray, *J. Am. Chem. Soc.* **1998**, *120*, 9396 – 9397.
[12] a) T. Teranishi, M. Miyake, *Chem. Mater.* **1998**, *10*, 594 – 600; b) T. Teranishi, I. Kiyokawa, M. Miyake, *Adv. Mater.* **1998**, *10*, 596 – 599; c) T. Teranishi, M. Hosoe, T. Tanaka, M. Miyake, *J. Phys. Chem. B* **1999**, *103*, 3818 – 3827.
[13] a) G. W. Busser, J. G. van Ommen, J. A. Lercher in *Advanced Catalysts and Nanostructured Materials*: *Modern Synthetic Methods* (Ed.: W. R. Moser), Academic Press, San Diego, **1996**, pp. 213 – 230; b) G. W. Busser, J. G. van Ommen, J. A. Lercher, *J. Phys. Chem. B* **1999**, *103*, 1651 – 1659; c) H. Hirai, Y. Nakao, N. Toshima, *J. Macromol. Sci. Chem.* **1979**, *13*, 727 – 750.
[14] a) R. G. DiScipio, *Anal. Biochem.* **1996**, *236*, 168 – 170; b) K. Esumi, M. Shiratori, H. Ishizuka, T. Tano, K. Torigoe, K. Meguro, *Langmuir* **1991**, *7*, 457 – 459.
[15] a) O. Vidoni, K. Philippot, C. Amiens, B. Chaudret, O. Balmes, J.-O. Malm, J.-O. Bovin, F. Senocq, M.-J. Casanove, *Angew. Chem.* **1999**, *111*, 3950 – 3952; *Angew. Chem. Int. Ed.* **1999**, *38*, 3736 – 3738; b) A. Duteil, R. Quéau, B. Chaudret, R. Mazel, C. Roucau, J. S. Bradley, *Chem. Mater.* **1993**, *5*, 341 – 347.
[16] a) G. Schmid, *Inorg. Synth.* **1990**, *27*, 214 – 218; b) M. N. Vargaftik, V. P. Zagorodnikov, I. P. Stolarov, I. I. Moiseev, D. I. Kochubey, V. A. Likholobov, A. L. Chuvilin, K. I. Zamaraev, *J. Mol. Catal.* **1989**, *53*, 315 – 348.
[17] a) D. H. Rapoport, W. Vogel, H. Cölfen, R. Schlögl, *J. Phys. Chem. B* **1997**, *101*, 4175 – 4183; b) D. van der Putten, R. Zanoni, C. Coluzza, G. Schmid, *J. Chem. Soc. Dalton Trans.* **1996**, 1721 – 1725.
[18] M. T. Reetz, M. Maase, *Adv. Mater.* **1999**, *11*, 773 – 777.
[19] a) M. T. Reetz, W. Helbig, *J. Am. Chem. Soc.* **1994**, *116*, 7401 – 7402; b) J. Becker, R. Schäfer, R. Festag, W. Ruland, J. H. Wendorff, J. Pebler, S. A. Quaiser, W. Helbig, M. T. Reetz, *J. Chem. Phys.* **1995**, *103*, 2520 – 2527; c) M. T. Reetz, W. Helbig, S. A. Quaiser in *Active Metals*: *Preparation*, *Characterization*, *Applications* (Ed.: A. Fürstner), VCH, Weinheim, **1996**, pp. 279 – 297.
[20] a) N. Ibl, *Chem.-Ing.-Tech.* **1964**, *36*, 601 – 612; b) R. Walker, *Chem. Ind.* **1980**, 260 – 264.
[21] a) H. Natter, T. Krajewski, R. Hempelmann, *Ber. Bunsenges. Phys. Chem.* **1996**, *100*, 55 – 64; b) H. Natter, R. Hempelmann, *J. Phys. Chem.* **1996**, *100*, 19525 – 19532; c) J. V. Zoval, R. M. Stiger, P. R. Biernacki, R. M. Penner, *J. Phys. Chem.* **1996**, *100*, 837 – 844; d) T. M. Whitney, J. S. Jiang, P. C. Searson, C. L. Chien, *Science* **1993**, *261*, 1316 – 1319, e) L. Xu, W. L. Zhou, C. Frommen, R. H. Baughan, A. A. Zakhidov, L. M. Malkinski, J.-Q. Wang, J. B. Wiley, *Chem. Commun.* **2000**, 997 – 998; f) P. N. Bartlett, P. R. Birkin, M. A. Ghanem, *Chem. Commun.* **2000**, 1671 – 1672.
[22] M. A. Winter, *Dissertation*, Ruhr-Universität Bochum, Germany, **1998**.
[23] G. R. Strobl, *Acta Crystallogr. Sect. A* **1970**, *26*, 367 – 375.
[24] M. T. Reetz, W. Helbig, S. A. Quaiser, U. Stimming, N. Breuer, R. Vogel, *Science* **1995**, *267*, 367 – 369.
[25] *Small-angle X-ray Scattering* (Eds.: O. Glatter, O. Kratky), Academic Press, London, **1982**.
[26] A. Guinier, *X-ray Diffraction in Crystals*, *Imperfect Crystals*, *and Amorphous Bodies*, Freeman, San Franscisco, **1963**.
[27] C. Reichardt, *Solvents and Solvent Effects in Organic Chemistry*, 2nd ed., VCH, Weinheim, **1988**.
[28] a) Southhampton Electrochemistry Group, *Instrumental Methods in Electrochemistry*, Ellis Horwood, Chichester, **1990**; concerning the mechanism of electrochemically induced metal powder production, see also: b) B. E. Conway, J. O'M. Bockris, *Proc. R. Soc. London Ser. A* **1958**, *248*, 394 – 403.
[29] We thank a referee for pointing this out.
[30] a) J. W. Niemantsverdriet, *Spectroscopy in Catalysis*: *An Introduction*, VCH, Weinheim, **1993**; b) V. Gnutzmann, W. Vogel, *J. Phys. Chem.* **1990**, *94*, 4991 – 4997; c) W. Vogel, J. S. Bradley, O. Vollmer, I. Abraham, *J. Phys. Chem. B* **1998**, *102*, 10853 – 10859.
[31] a) W. Vogel, B. Rosner, B. Tesche, *J. Phys. Chem.* **1993**, *97*, 11611 – 11616; b) W. Vogel, *Crystallogr. Res. Technol.* **1998**, *33*, 1141 – 1154.
[32] The incorporation of carbon and/or oxygen in Pd nanoparticles has been reported to increase the Pd–Pd distance: a) N. Krishnankutty, M. A. Vannice, *J. Catal.* **1995**, *155*, 312 – 326; b) K. Okitsu, Y. Mizukoshi, H. Bandow, T. A. Yamamoto, Y. Nagara, Y. Maeda, *J. Phys. Chem. B* **1997**, *101*, 5470 – 5447; c) M. Maciejewski, A. Baiker, *Pure Appl. Chem.* **1995**, *67*, 1879 – 1884; d) J. W. M. Jacobs, D. Schryvers, *J. Catal.* **1987**, *103*, 436 – 449.
[33] A. Yasuhara, A. Kasano, T. Sakamoto, *Organometallics* **1998**, *17*, 4754 – 4756.
[34] a) J. A. Becker, R. Schäfer, R. Festag, W. Ruland, J. H. Wendorff, J. Pebler, S. A. Quaiser, W. Helbig, M. T. Reetz, *J. Chem. Phys.* **1995**, *103*, 2520 – 2527; b) J. A. Becker, R. Schäfer, R. Festag, J. H. Wendorff, F. Hensel, J. Pebler, S. A. Quaiser, W. Helbig, M. T. Reetz, *Surf. Rev. Lett.* **1996**, *3*, 1121 – 1126; c) M. T. Reetz, S. A. Quaiser, M. Winter, J. A. Becker, R. Schäfer, U. Stimming, A. Marmann, R. Vogel, T. Konno, *Angew. Chem.* **1996**, *108*, 2228 – 2230; *Angew. Chem. Int. Ed. Engl.* **1996**, *35*, 2092 – 2094.
[35] M. T. Reetz, S. A. Quaiser, C. Merk, *Chem. Ber.* **1996**, *129*, 741 – 743.
[36] a) Y.-Y. Yu, S.-S. Chang, C.-L. Lee, C. R. C. Wang, *J. Phys. Chem. B* **1997**, *101*, 6661 – 6664; see also b) M. B. Mohamed, Z. L. Wang, M. A. El-Sayed, *J. Phys. Chem. A* **1999**, *103*, 10255 – 10259.
[37] M. T. Reetz, W. Helbig, S. A. Quaiser, *Chem. Mater.* **1995**, *7*, 2227 – 2228.
[38] M. T. Reetz, S. A. Quaiser, *Angew. Chem.* **1995**, *107*, 2461 – 2463; *Angew. Chem. Int. Ed. Engl.* **1995**, *34*, 2240 – 2241.
[39] This colloid was prepared by a modified version of the electrochemical procedure based on metal salts,[37] water being used in place of acetates.[22]
[40] Size selectivity in the preparation of polymer-stabilized Pd/Ni colloids has recently been achieved by treating preformed Pd colloids with nickel salts under chemically reducing conditions: T. Teranishi, M. Miyake, *Chem. Mater.* **1999**, *11*, 3414 – 3416.

Received: May 08, 2000 [F2469]

  0947-6539/01/0705-1094 $ 17.50+.50/0